Int. J. Electrochem. Sci., 8 **(2013)** 12192 - 12204

International Journal of
ELECTROCHEMICAL
SCIENCE
www.electrochemsci.org

Influence of Constant Magnetic Field on the Electrodeposition of Cobalt and Cobalt Alloys

Marek Zieliński

Department of Inorganic and Analytical Chemistry, Faculty of Chemistry, University of Lodz, Tamka 12, 91-403 Lodz, Poland
E-mail: zielmark@chemia.uni.lodz.pl; magnet@toya.net.pl

Received: 7 August 2013 / *Accepted:* 29 August 2013 / *Published:* 25 September 2013

The paper presents a study of the effect of constant magnetic field (CMF) on the basic processes of Co-Mo, Co-W, Co-Mo-W alloys and Co electrodeposition. The applied research methods included scanning electron microscopy (SEM), energy dispersive X-ray (EDX) microanalysis, cyclic voltammetry (CV), coulometry (C), scanning tunneling microscope (STM) and X-ray diffraction (XRD). SEM images of Co-Mo, Co-W, Co-Mo-W alloys revealed numerous fractures on the samples surface, formed as a result of residual stress during alloy deposition without CMF. In CMF such fractures disappeared. Under CMF conditions some crystal planes were deflected at angles ranging from 15 to 20º. The exposure to CMF caused also an increase of the volume fraction (by about 10 % by volume) of the dominant phase in the alloys. The reason for these changes was the fact that the Lorentz force, generated in CMF, caused the magnetohydrodynamic (MHD) effect. This induced movement of the electrolyte. The Nernst diffusion layer was depleted, whereas a new Navier-Stokes hydrodynamic layer appeared, which determined the velocity of electroactive molecules flow to the working electrode under CMF conditions.

Keywords: Cobalt, Alloys, Electrodeposition, Constant magnetic field

1. INTRODUCTION

Cathodic electrodeposition of alloys based on elements belonging to the ferrous metals group (Fe, Co, Ni) is still an important problem in electrochemistry. Studies on alloys have focussed on what are known as functional metallic layers characterised by specific physicochemical properties, including mechanical, electrical, magnetic and optical. Codeposition of the mentioned elements with metals such as chromium, molybdenum and tungsten, or non-metals such as phosphorus and boron is an interesting issue. They are elements which cannot be deposited from aqueous solutions alone, but only in the

presence of ferrous metals by the so-called induced codeposition. Hamid [1] studied the optimal conditions for cobalt-tungsten alloy electrodeposition process, such as temperature, current density, concentration of metal ions or surfactants. Then, he investigated the morphology of alloy surfaces, their microhardness and resistance to corrosion. With tungsten content ranging from 3 to 10% by weight, the alloy had a fine-grained structure, whereas when tungsten content increased to 15% by weight, the structure of the alloy was fibrous with even finer grains. Chang et al. [2] demonstrated that higher tungsten content in cobalt-tungsten alloys improved their corrosion resistance. Shobba et al. [3] studied the corrosion resistance of alloys exposed to sulfuric acid (VI) and potassium hydroxide. The study was carried out in the context of applicability of these alloys as anode materials. It had been observed earlier that magnetic field may affect electrochemical processes [4–6]. The obtained data indicated that such changes are due to magnetohydrodynamic (MHD) effect. The MHD effect is based on the Lorentz force, inducing movements of the electrolyte and increasing or decreasing transport of the electroactive molecules to the electrode. Koza et al. [7] studied the effect of constant magnetic field (CMF) with magnetic induction value ranging from zero do 1 T, in various configurations in relation to the electrode surface. They observed that CMF applied parallel to the electrode surface increased the limiting current density and the deposition rate. This was due to the MHD effect, induced by maximal Lorentz force generated in the hydrodynamic layer. They deposited electrochemically cobalt, iron and cobalt-iron alloy [7-9]. Matsushima et al. [10] reported that grains of Fe electrodeposited without the influence of a magnetic field had sharp ends, and their sizes were larger than grains electrodeposited in a magnetic field, the latter being rounded. Msellak et al. [11] proved that Ni-Fe alloys deposited in a magnetic field with an induction of 0.9 T were smoother, had a uniform structure and featured a preferential grain orientation. Coey and Hinds [12] confirmed that CMF increased significantly copper electrodeposition rate. Then, they observed increased transport of cationic mass, both diamagnetic (Ag^{+}, Zn^{2+}, Bi^{3+}) and paramagnetic (Cu^{2+}, Ni^{2+}) under CMF conditions. O'Reilly et al. [13] found that under the influence of a CMF, an increase in the current density ($\boldsymbol{j}$) occurred, caused by the decreasing thickness of the diffusion layer (δ_D). Lioubashevski et al. [14, 15] developed a theoretical hydrodynamic model demonstrating the influence of a magnetic field on electrochemical processes. Moreover, they defined an empirical formula for calculating the value of current depending on the magnetic induction applied: $i \approx C^{3/4} \cdot B^{1/3}$. Ragsdale and White [16,17] showed microscopic images confirming magnetohydrodynamic flow in the electrolyte, demonstrating that the flow is more intense when the direction of vector ($\boldsymbol{B}$) is parallel to the working electrode surface than when it is perpendicular to the working electrode surface. In this paper, the effect of CMF on electrodeposition of Co-Mo, Co-W, Co-Mo-W alloys and Co has been studied. The results obtained show that the application of CMF causes changes in the kinetics of alloy deposition reactions, changes in the chemical composition of the alloys and their surface morphology, as well as changes in the crystallographic parameters of the alloys.

2. EXPERIMENTAL PART

Co-Mo, Co-W, Co-Mo-W alloys and Co were prepared by electrodeposition using three-electrode system. The three-electrode electrochemical cup, in which the alloys were deposited,

consisted of a working electrode (gold, disc-shaped) with 0.1 cm^2 surface area, an auxiliary electrode (platinum, mesh) and a reference electrode (saturated, calomel) (SCE).

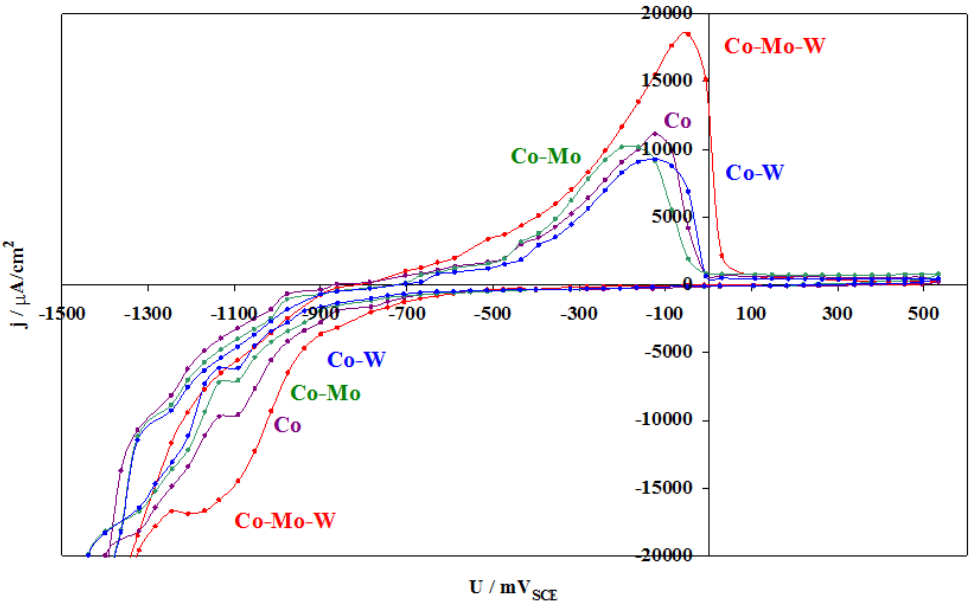

Figure 1. Cyclic voltammogram of Co-Mo, Co-W, Co-Mo-W alloys and Co.

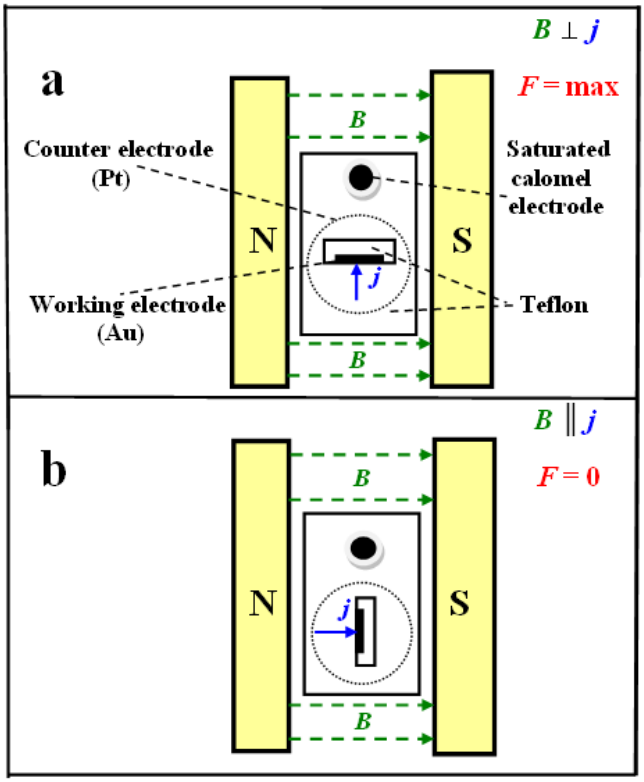

Figure 2. Electrochemical cup with three-electrode measurement system, placed between the N and S pole pieces of a laboratory electromagnet, (a) with the magnetic induction *B* perpendicular to the current density *j*, and (b) with the magnetic induction *B* parallel to the current density *j*. *F* denotes the Lorentz force.

The galvanic solution prepared to obtain Co-Mo, Co-W, Co-Mo-W alloys and Co contained 0.1M cobalt sulfate ($CoSO_4 \cdot 7H_2O$), 0.1M sodium molybdate ($Na_2MoO_4 \cdot 2H_2O$), 0.1M sodium tungstate ($Na_2WO_4 \cdot 2H_2O$), 0.6M sodium citrate ($Na_3C_6H_5O_7 \cdot 2H_2O$), 0.05 M EDTA ($C_{10}H_{14}O_8N_2Na_2 \cdot 2H_2O$) and 0.1M sulfuric acid (H_2SO_4). The Co-Mo, Co-W, Co-Mo-W alloys and Co electrodeposition potential was determined on the basis of the dependence of current on potential - cyclic voltammetry methods (CV) (Figure 1).

The Co-Mo, Co-W, Co-Mo-W alloys and Co were deposited without and in CMF produced by the N and S pole pieces of an ER 2525 laboratory electromagnet. The magnetic induction *B*, used in the study within the value range from zero to 1200 mT, was directed either parallel to the surface of the working electrode (i.e. perpendicular to the current density ***j*** direction, $\boldsymbol{B} \perp \boldsymbol{j}$ configuration), or perpendicular to the surface of the working electrode (i.e. parallel to the current density ***j*** direction, $\boldsymbol{B} \parallel \boldsymbol{j}$ configuration), as presented in Figure 2.

The morphological structure of the alloys was studied by SEM using a Philips XL 30 instrument. Images were recorded in the backscattered electron or secondary electron mode at 10 keV or 20 keV primary beam energy. The chemical composition of the alloys was determined by energy dispersive X-ray (EDX) microanalysis using an Oxford Instruments ISIS system. The crystallographic structure of the alloys was studied by XRD using a Bruker D8 Discover X-ray diffractometer with a Cu K_α radiation. By STM topography of the surface alloys was analyzed. The parameters of the STM test were as following: the measurements were made in air; the Pt (90) Ir (10) needle was an electrochemically etched; the voltage 'needle – test sample' was E_T = + 0,2 V; tunnel current was I_T = + 10 nA.

3. RESULTS AND DISCUSSIONS

Electrodeposition is a remarkably versatile (and inexpensive) method of preparing metallic films and nanostructures, including those made of ferromagnetic metals and alloys. There are two possible sources of the magnetic force acting on the electrochemical system and responsible for the observed magnetic field effects. The first is related to the movement of charged species and the second is related to the magnetic properties of the electrochemically active substrate. The first type of magnetic body force is the Lorentz force, *F* (1), acting on the unit volume of charge-carrying ions and resulting in a momentum transfer to the solvent that could result in the field driven solution flow:

$$F = j \times B \qquad (1)$$

where *j* is the current density and *B* is the magnetic induction.

On the basis of the coulometry (C) measurements, the relationship between the charge (*Q*) flowing in the electrolyte and magnetic induction (*B*) were determined for Co, specific Co-Mo, Co-W and Co-Mo-W alloys. Figure 3 indicates that the more complicated the structure of the metallic coating, i.e. Co, Co-Mo, Co-W, Co-Mo-W, the higher the value of magnetic induction (*B*) required to achieve maximum effect of the CMF on the charge (*Q*).

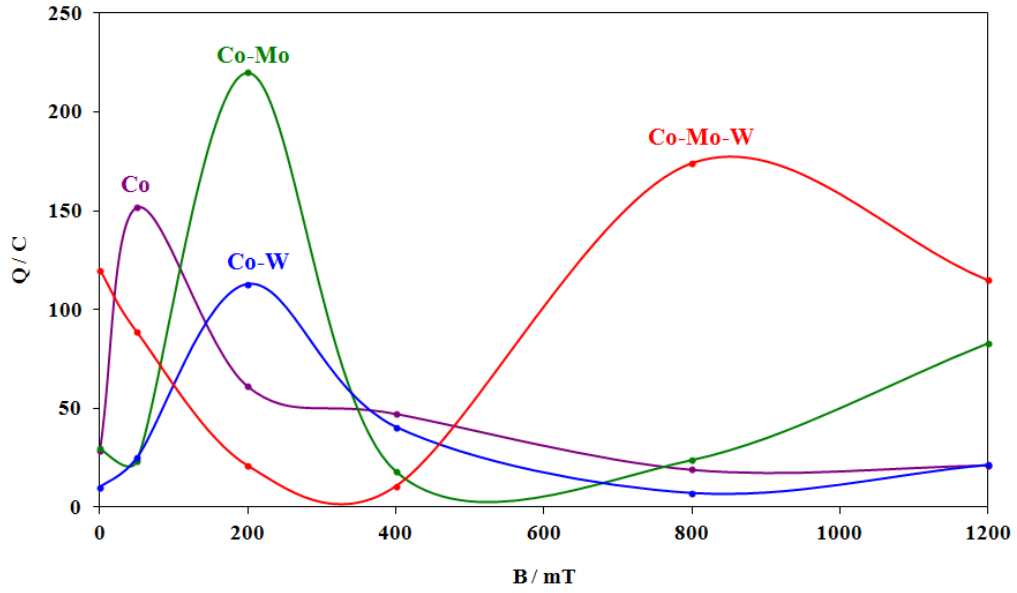

Figure 3. The relationship between the charge (Q) and magnetic induction (B) during the electrodeposition reaction of Co and Co-Mo, Co-W and Co-Mo-W alloys.

For the fluid that contains electroactive para- or diamagnetic species, the magnetization, M, induced by the field, B, depends on the local value of the applied magnetic field as well as on the molar magnetic susceptibility, χ_m, of these species, which is proportional to their concentration. A concentration gradient of the magnetic species, created as a result of the heterogeneous electrochemical reaction, produces a spatial variation in the magnetization through the molar magnetic susceptibility, and therefore results in the spatially nonuniform magnetic body force density. This magnetic body force can promote or inhibit convection in a manner similar to the gravitational body force. The density of the magnetostatic energy of the electrolyte containing magnetic species in the magnetic field is given by the following Eq. (2)

$$E_{mag} = -1/2\mu_0 MB = -1/2\mu_0 \chi_m CB^2 \qquad (2)$$

where M is the magnetization induced by the field B, μ_0 is the magnetic permeability of free space, and χ_m, is the molar magnetic susceptibility of the species involved. To calculate the force associated with this magnetic energy, we have to take a spatial derivative of the energy (3)

$$F_{mag} = -\nabla E = 1/2\nabla\left(\chi_m CB^2\right) \qquad (3)$$

Magnetic force acting on the electrolyte, that contains magnetic species, due to the magnetic energy gradient, is given by Eq. (4)

$$F_{mag} = \frac{\chi_m B^2 \nabla C}{2\mu_0} + \frac{\chi_m CB\nabla B}{\mu_0} \qquad (4)$$

where ∇B is the magnetic field gradient. This force includes two terms: the concentration gradient force, F_C (Kelvin body force) and the field gradient force, F_B. The concentration gradient force, F_C, is directed toward areas with higher concentration of the paramagnetic species and the field gradient force, F_B, is directed toward areas with higher values of the magnetic field strength, Eq. (5)

$$F_{mag} = F_C + F_B \quad (5)$$

An induced ion transport direction depends on the sign of the product of the magnetic susceptibility and the concentration gradient, defined by which electroactive component possesses magnetic properties, the substrate or product of the electrochemical reaction. The negative sign means that the flow directed toward the electrode surface and the positive sign means the outward flow. The direction of the magnetic field is irrelevant to the direction of F_C because the magnetic flux density in equation (4 and 5) relates to the second power of the strength of the magnetic field, B^2. The field gradient force, F_B, has the direction defined by the product of the magnetic field and the gradient of the magnetic field and the magnetic susceptibility of the ions.

The morphology of the alloys was studied using SEM. The Co-Mo, Co-W, Co-Mo-W alloys and Co were obtained electrochemically either with no exposure to magnetic field or under CMF conditions. Such studies ran Msellak et al. [11], but for the Ni-Fe alloy, in CMF of the magnetic induction B = 0.9 T. The SEM studies showed the presence of numerous fractures in the central portion of the samples surface, formed as a result of residual stress during alloy deposition without CMF (Figure 4). With CMF value B = 1200 mT and $\boldsymbol{B} \perp \boldsymbol{j}$ configuration, such fractures disappeared.

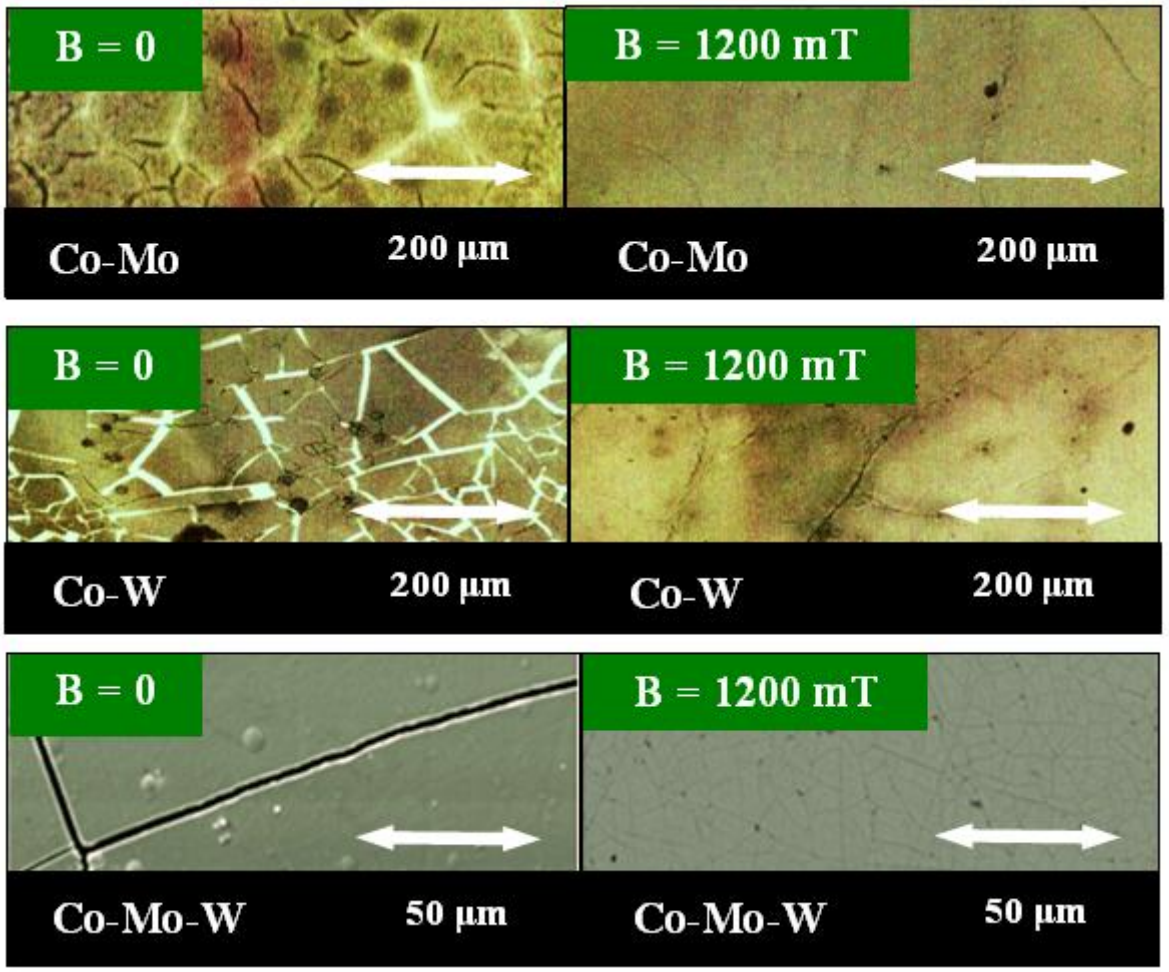

Figure 4. Reduction in fracture widths on the surface of Co-Mo, Co-W and Co-Mo-W alloy under the influence of a CMF.

Lioubashevski et al. [14] has formulated a quantitative theoretical model that accounts for the constant magnetic field effect on electrochemical reactions. The cornerstone of the model is relation between the thickness of the Nernst diffusion layer (δ_D) and magnetic induction (B). The equation 6 is a modification thereof:

$$\delta_D \approx 1.59(\rho R \nu^{2/3} D^{1/3})^{1/3} (nF_F CB)^{-1/3} \qquad 6)$$

where R is radius of the working disk electrode, n is the number of electrons involved in the Faradaic process, $F_F = 96487$ C·mol^{-1} is the Faraday's number, C is the concentration of electroactive ions in the body of the electrolyte, D is the electrolyte diffusivity, ν is the bulk flow velocity and ρ is the fluid specific density.

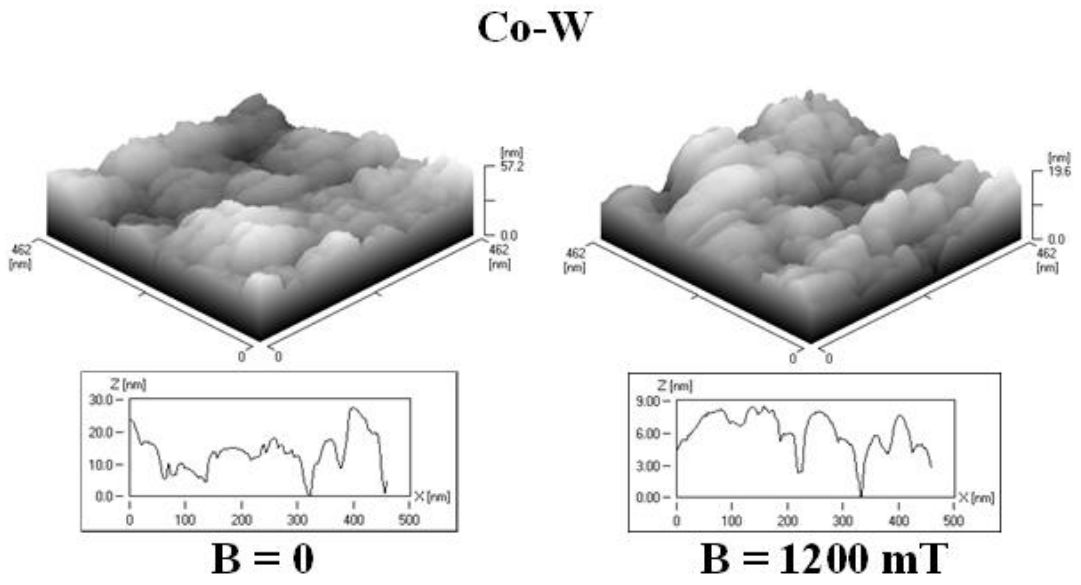

Figure 5. STM. Surface topography of gold plate electrodes electrochemically coated with Co-W over scanning area (462×462nm) in presence of magnetic induction B = 0 and B = 1200 mT.

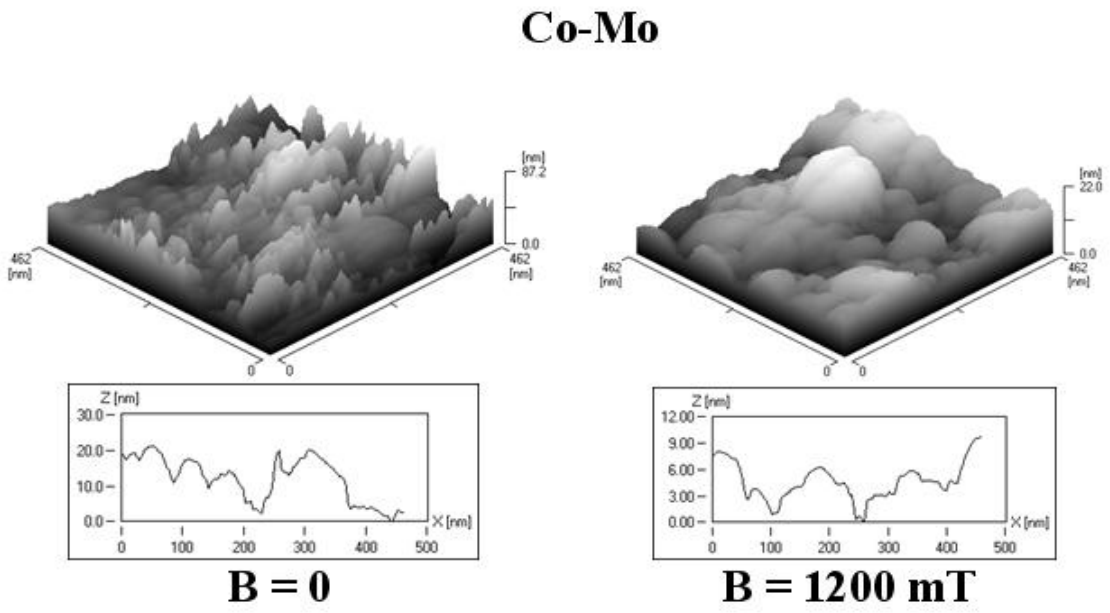

Figure 6. STM. Surface topography of gold plate electrodes electrochemically coated with Co-Mo over scanning area (462×462nm) in presence of magnetic induction B = 0 and B = 1200 mT.

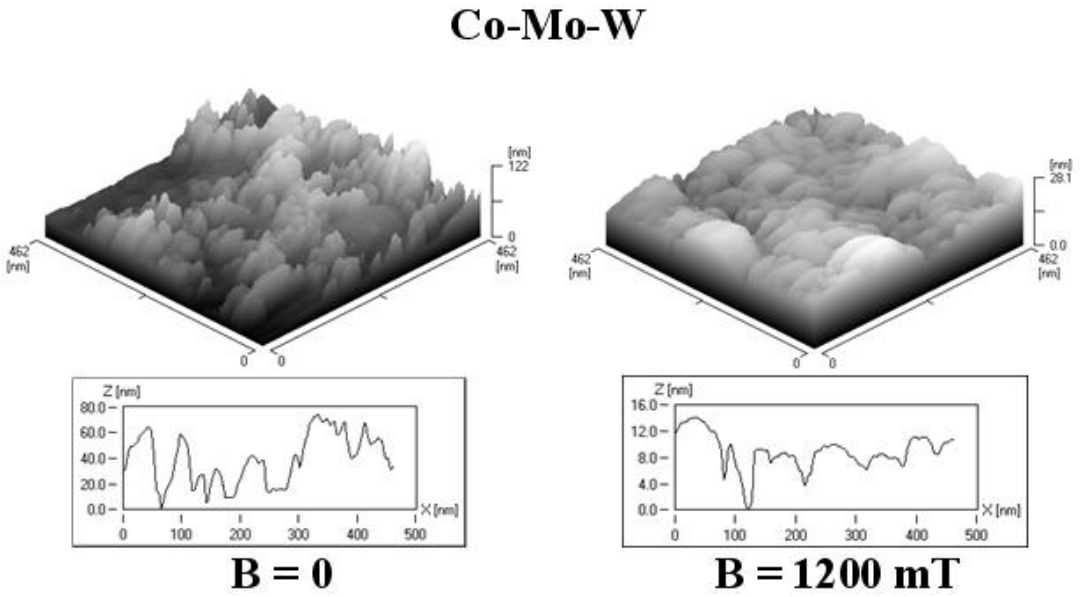

Figure 7. STM. Surface topography of gold plate electrodes electrochemically coated with Co-Mo-W over scanning area (462×462nm) in presence of magnetic induction B = 0 and B = 1200 mT.

Consequently, the concentration of electroactive ions (C_{el}) at the electrode increased and a larger amount of the alloy was deposited:

$$m \approx 0.63(\rho R)^{-1/3} \nu^{-2/9} D^{8/9} (nF_F CB)^{1/3} \qquad (7)$$

where m is mass of alloy.

Leventis et al. [18] examining the effect of magnetic field in the electrochemical reactions, in a magnetic field having a remanence of from 0.8 to 1.8 T, tagged weight gain of organic compounds by using CMF.

The magnetic field applied during the deposition of alloy layers from the electrolyte, reduces the layers internal stress. The tensile stress in alloys films obtained with applied magnetic field is lower than in those deposited in the absence of a magnetic field. When a magnetic field is applied parallel to the electrode surface, the deposits look more homogeneous than those deposited without field. It is also visible that the deposits obtained in the parallel magnetic field are more densely packed and possess smaller porosity (Figures 5-7). This was confirmed in his research Matsushima et al. [10]. Electrochemically deposited on iron during operation CMF with magnetic induction from 0 to 5 T. On the basis of the data recorded with EDX microanalysis in the scanning electron microscope (SEM), the percentage contents of cobalt, molybdenum and tungsten in the investigated alloys were determined. They were deposited with no exposure to magnetic field and in CMF with magnetic induction values B = 200, 600 and 1200 mT. The obtained results are presented in Figure 8.

The phase structure and crystalline lattice parameters of the investigated alloys were determined by the XRD method. The phases were identified on the basis of the experimental data recorded using the XRD technique in asymmetric geometry 2θ-scan, with EVA software [19] as well as the data obtained from ICDD crystallographic database. The analysis of dominant phase texture (phase volume fractions) in the alloy coatings was based on experimental so-called pole figures with application of thin layer correction. Decreased intensity of the reflected beams indicated that under

CMF conditions some crystal planes were deflected at a specific angle during the alloy formation process. The higher the value of magnetic induction, the more significant deflection of some crystal planes took place.

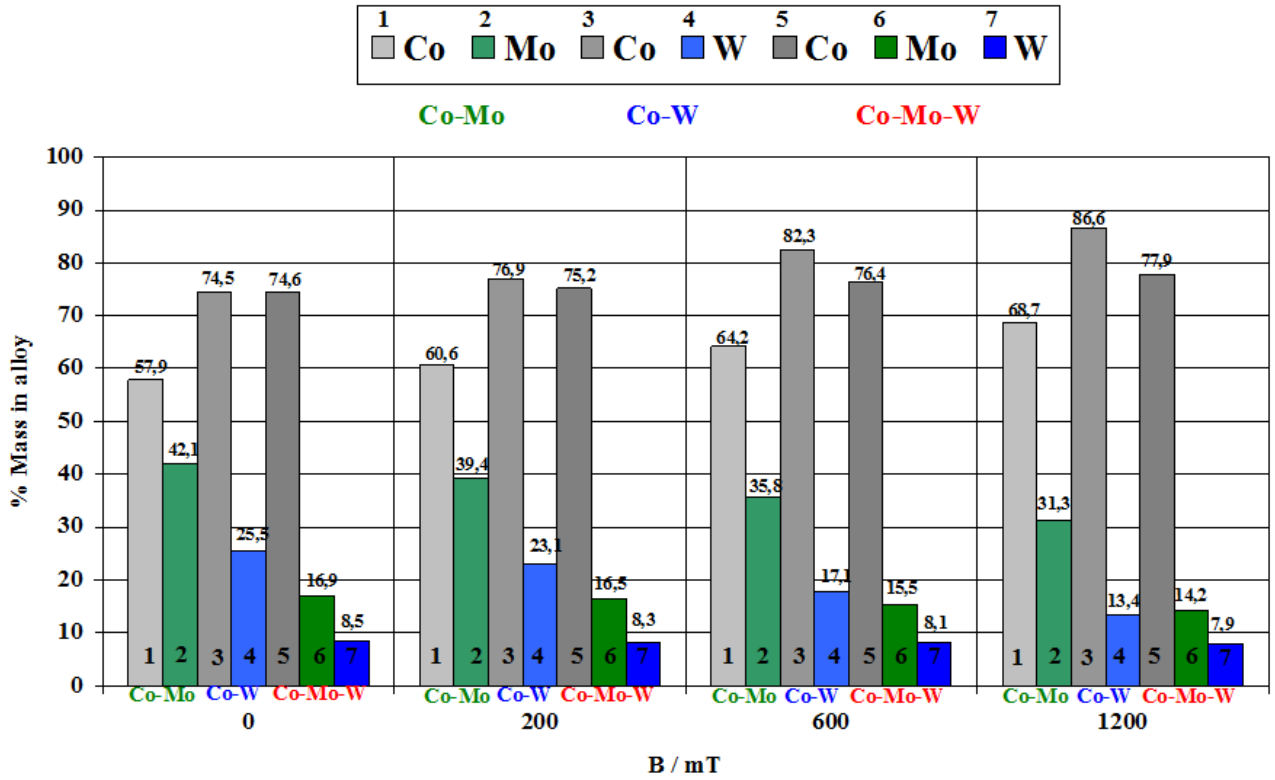

Figure 8. Composition of alloys obtained from these electrolytes both with and without a CMF, examined using EDX.

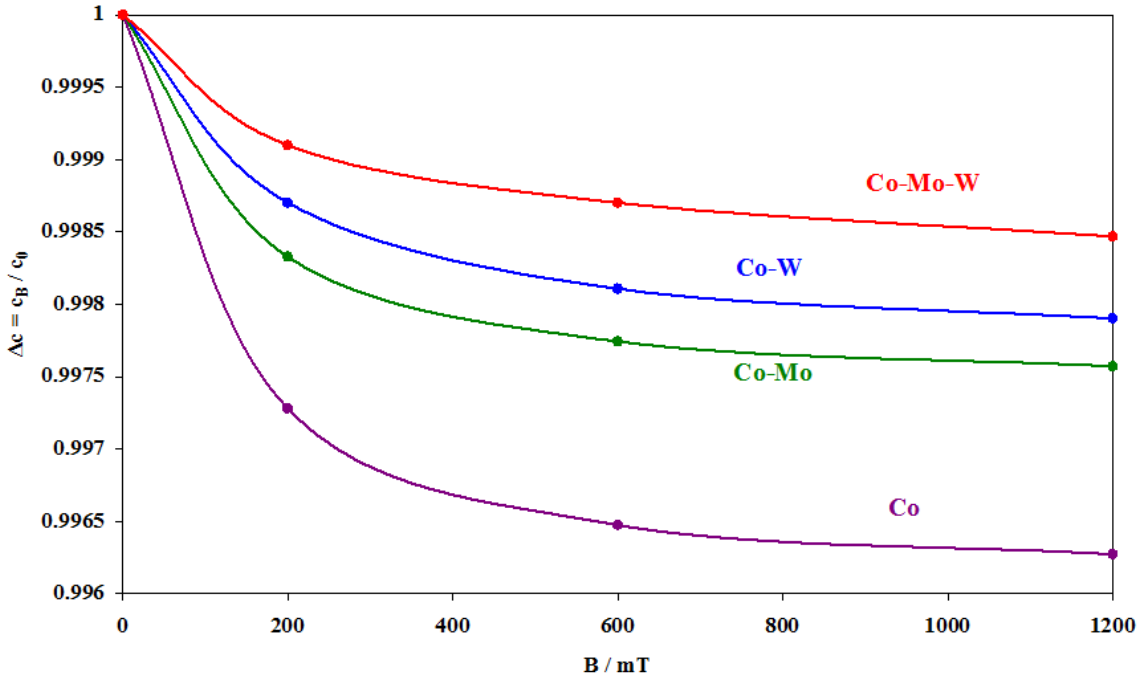

Figure 9. The relationship between Δ*c* and *B* of Co and Co-Mo, Co-W, Co-Mo-W alloys.

The lattice parameter *c* was taken into account in the conducted measurements as a characteristic parameter for the studied case. As a result of the exposure to CMF, Co and Co-Mo, Co-W, Co-Mo-W alloys crystals were more flattened, which is confirmed by the decreasing lattice parameter *c* of the dominant phase (Figure 9). Calculated change network parameter *c* as:

$$\Delta c = \frac{c_B}{c_0} \qquad 8)$$

where: c_B - crystalline lattice parameters *c* in a CMF,

c_0 - crystalline lattice parameters *c* without field

The spatial disposition for example of Co_3W and Co_7W_6 phase crystallites in the analyzed coating layers demonstrated a tendency towards formation of {0 0 0 1} type (basal) lattice planes, slightly deflected - by 15^o – 20^o - in relation to the external sample surface plane. The precise orientation of crystallites should be described as a {0 -1 1 3} type plane, parallel to the external sample surface. The above tendency was the most pronounced in sample 1 (*B* = 0) and weaker in samples 2, i.e. in those exposed to CMF (*B* = 1200 mT) had been used with $\boldsymbol{B} \perp \boldsymbol{j}$ (Figure 10).

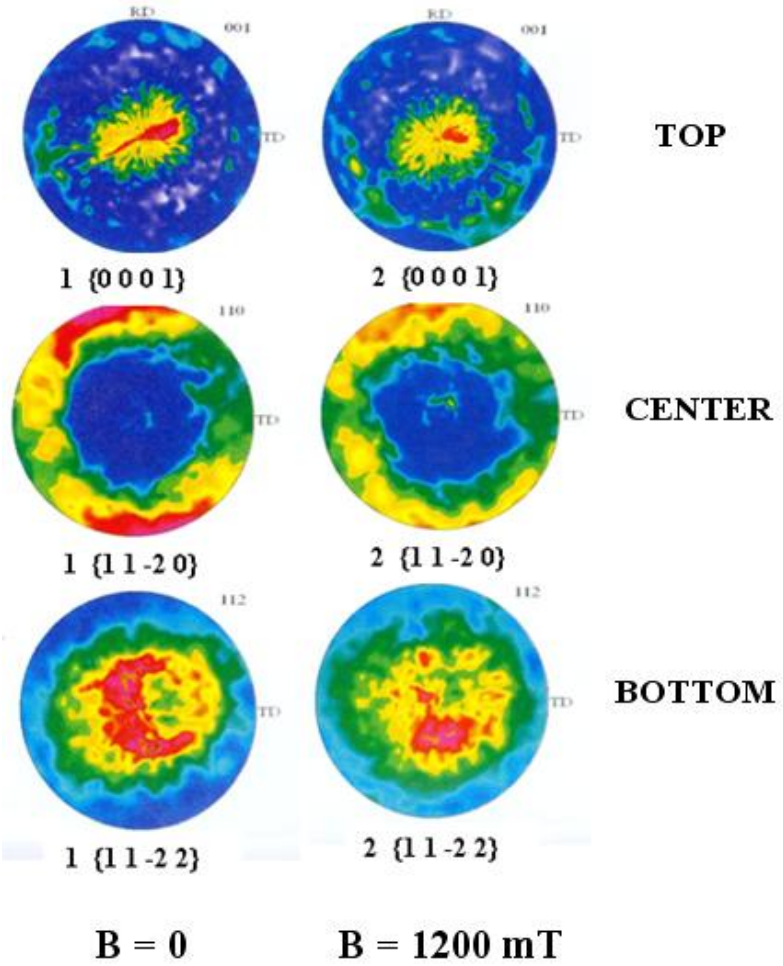

Figure 10. Pole figures for the basal planes of {0 0 0 1} type (top), prismatic ones of {1 1 –2 0} type (center) and pyramidal ones of {1 1 –2 2} type (bottom) of the hexagonal phase Co_3W in cobalt-tungsten alloy samples 1 and 2.

The most important effect of CMF on electrochemical processes is the MHD effect. The driving force of that effect is the generated Lorentz force F (1). In the case of configuration $\boldsymbol{B} \perp \boldsymbol{j}$, this is a macroscopic effect. It causes additional convection, resulting in an increase of mass transport towards the working electrode. Consequently, a laminar flow of electrolyte near the working electrode surface occurs, reducing the diffusion layer thickness and causing an increase of potential-generating ions concentration. It causes a change of grain size in the deposited alloy, affects its texture and formation of various phases. Such effects are caused by additional convection, as well as by the magnetic properties of ions. Hinds et al. studied the formation of additional diffusion under the influence of CMF about magnetic induction from 0 to 6 T. Deposition of Cu from $CuSO_4$ a solution of with a concentration of 0.75 M. How to they wrote in their paper [20], effect of the CMF on the morphology of the deposited copper can be directly related to the modified mass transport rate. Ionic mass transfer can be extended by convection and consequently one can define the phenomenon as convective diffusion. There is a solution layer of thickness δ_D (Nernst diffusion layer) between the working electrode surface and the electrolyte mass, the mass transfer through which occurs only as a result of diffusion and migration. The layer thickness δ_D is dependent on hydrodynamic conditions and viscosity of the solution.

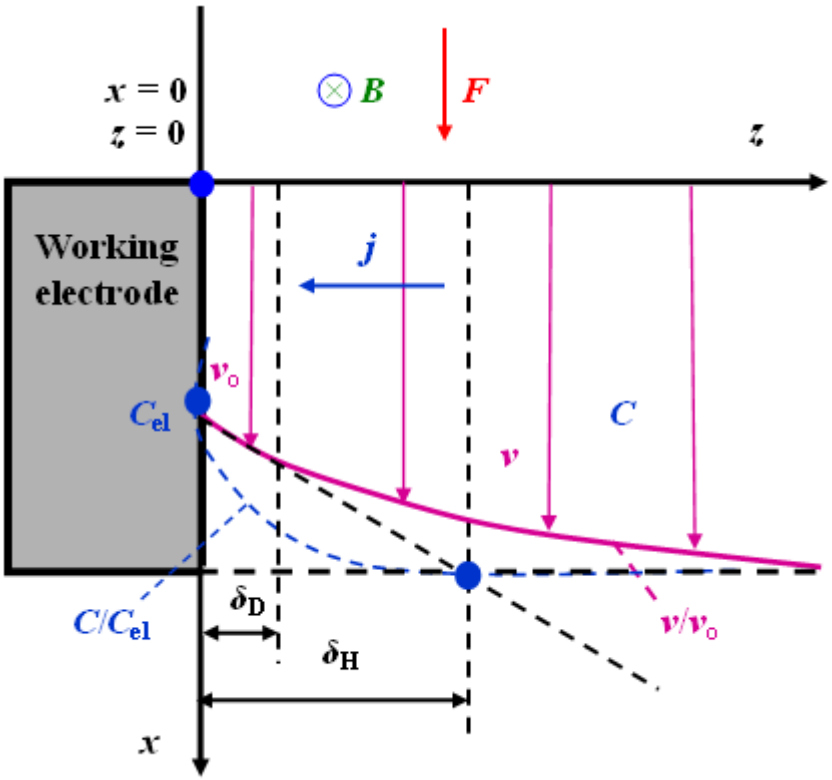

Figure 11. Reduction in the Nernst diffusion layer thickness δ_D near the working electrode surface under the influence of CMF, and formation of the Navier-Stokes hydrodynamic layer δ_H.

There is a gradient of concentrations $(C - C_{el})$ in the aforementioned diffusion layer δ_D; thus, the mass diffusion transfer J_{diff} can be written as:

$$J_{diff} = D(C - C_{el}) / \delta_D \qquad (9)$$

The rate of reduction of electroactive ions on the working electrode surface is higher than the rate of reagents supply, thus mass transport in the diffusion layer can be expressed as follows:

$$C_{el} = 0\,|_{z=0} \quad \text{and} \quad C_{el} = C\,|_{z\to\infty} \qquad (10)$$

where *z* is the perpendicular direction from the electrode surface.

The force *F* generated as a result of the exposure to CMF caused electrolyte movements. The Nernst diffusion layer δ_D was depleted, while a new Navier-Stokes hydrodynamic layer δ_H appeared (Figure 11). In accordance with theoretical considerations, the Lorentz magnetic forces under the experimental conditions resulted in the motion of the electrolyte being tangential to the working electrode surface and perpendicular to the magnetic induction vector, ***B***. A laminar and unidirectional (x-direction) flow of electrolyte was assumed. A Navier-Stokes hydrodynamic layer (δ_H) was formed, resulting in a reduction in the diffusion layer (δ_D). The presented considerations concerned obviously the flat surface of the working electrode, and the CMF was parallel to the working electrode surface.

It was also calculated that the velocity of electroactive molecules *v* increases with increasing magnetic induction *B*, as suggested in the article Lioubashevski et al. [15]. This relationship is represented by the equation 11:

$$v \approx \left(nF_F CD^{4/3} B\rho^{1/3}\delta_H\right)/\left(0.62\eta^{4/3}\right) \qquad (11)$$

where η is the dynamic viscosity.

With increasing magnetic induction *B*, the thickness of Navier-Stokes hydrodynamic layer δ_H, which determines the electrolyte flow under the exposure to CMF, also increases. A primary effect of magnetic fields on the electrochemical reaction is the MHD effect acting in the bulk electrolyte ($\boldsymbol{B} \perp \boldsymbol{j}$ configuration), which reduces the diffusion layer thickness and thus, the limiting current densities and deposition rates are increased with a superimposed magnetic field. The nucleation process is affected by the magnetic field when it is applied parallel to the electrode surface (maximal Lorentz force). This influence is attributed to the MHD effect. This is confirmed in their studies Bund and Kuehnlein [21]. They investigated oxidation and reduction reactions of Cu with 0.5 M CuSO4 solution, with the involvement CMF by magnetic induction from 0 to 0.8 T. No significant effect of magnetic fields on the electrochemical system was observed when they were applied perpendicular to the electrode surface. The investigation of magneto-electrolysis is of significance from both the industrial and fundamental points of view. It may open up a novel method of modifying the microstructure, in particular the particle content, by controlling the magnetic fields with no need to adjust additives and electrolyte composition.

4. CONCLUSION

The effect of CMF on the electrodeposition process of Co-Mo, Co-W, Co-Mo-W alloys and Co has been investigated. The results obtained show that the application of CMF causes changes in the kinetics of alloy deposition reactions, changes in the chemical composition of the alloys and their surface morphology, as well as changes in the crystallographic parameters of the alloys.

At present it seems that all the various effects of magnetic fields in electrochemistry are somehow related to mass transport. In the process of Co-Mo, Co-W, Co-Mo-W alloys and Co electrodeposition, the Lorentz force was generated as a result of the exposure to CMF. This force

induced MHD effects in the solution, thus causing electrolyte movements, with the resultant depletion of the Nernst diffusion layer and appearance of a new Navier-Stokes hydrodynamic layer, which determined the velocity of electroactive molecules flow to the working electrode. The coulometry method demonstrated that the more complicated the structure of metallic coating, the higher the value of magnetic induction (*B*) required for the CMF to achieve maximum influence on the charge value (*Q*). Under CMF conditions some crystal planes were deflected at a specific angle (ranging from 15 to 20º, depending on the value of magnetic induction) during the alloy formation process. The exposure to CMF changed also the volume fraction of the dominant phase in the alloy. It has been clearly demonstrated that the superimposition of magnetic fields influences significantly the resulting layer properties. A pronounced impact on the layer morphology has been observed. The layers deposited under the influence of the parallel-to-electrode magnetic field are denser and more homogeneous than those obtained without a magnetic field. New magnetic nanostructures can be produced using electrochemical scanning probe methods and a new level of control may be exerted over industrial catalytic and electroplating processes by appropriately designed field patterns.

ACKNOWLEDGMENTS
This work was supported by the Lodz University.

References

1. Z. A. Hamid, *Mater. Lett.*, 57 (2003) 2558-64.
2. J. Chang, J. Chou, R. Hsich and J. Lee, *Mat. Chem. Phys.*, 118 (2009) 314.
3. T. Shobba, S.M. Mayanna and C.A.C. Sequeira, *J. Power Sources*, 108 (2002) 261.
4. T.Z. Fahidy, *J. App. Electrochem.*, 13 (1983) 553.
5. T.Z. Fahidy, *Electrochim. Acta*, 18 (1973) 607.
6. R.A. Tacken and L.J.J. Janssen, *J. App. Electrochem.*, 25 (1995) 1.
7. J.A. Koza, M. Uhlemann, A. Gebert and L. Shultz , *Electrochim. Acta*, 53 (2008) 5344.
8. W. Szmaja, W. Kozłowski, K. Polański, J. Balcerski, M. Cichomski, J. Grobelny, M. Zieliński and E. Miękoś, *Mat. Chem. Phys.*, 132(2-3) (2012) 1060.
9. W. Szmaja, W. Kozłowski, K. Polański, J. Balcerski, M. Cichomski, J. Grobelny, M. Zieliński and E. Miękoś, *Chem. Phys. Lett*., 542 (2012) 117.
10. H. Matsushima, T. Nohira, J. Mogi and Y. Ito, *Surf. Coat. Technol.*, 179 (2004) 245.
11. K. Msellak, J.P. Chopart, O. Ibara, O. Aaboubi and J. Amblard , *J. Magn. Magn. Mater*., 281 (2004) 295.
12. J.M.D. Coey and G. Hinds, *J. Alloy Compd*., 326 (2001) 238.
13. C. O'Reilly, G. Hinds and J.M.D. Coey, *J. Electrochem. Soc*., 148(10) (2001) C674.
14. O. Lioubashevski, E. Katz and I. Willner, *J. Phys. Chem. B*, 108 (2004) 5778.
15. O. Lioubashevski, E. Katz and I. Willner, *J. Phys. Chem. C*, 111 (2007) 6024.
16. S.R. Ragsdale, K.M. Grant and H.S. White, *J. Am. Chem. Soc.*, 120 (1998) 13461.
17. S.R. Ragsdale and H.S. White, *Anal. Chem.*, 71 (1999) 1923.
18. N. Leventis, M. Chen, X. Gao, M. Canalas and P. Zhang, *J. Phys. Chem. B*, 102 (1998) 3512.
19. Software, Bruker AXS (2005).
20. G. Hinds, F. E. Spada, J.M.D. Coey, T.R.Ni Mhiochain and M.E.G. Lyons, *J. Phys. Chem. B*, 105 (2001) 9487.
21. A. Bund and H.H. Kuehnlein, *J. Phys. Chem. B*,109 (2005) 19845.